Mechanism study of alachlor biodegradation by *Paecilomyces marquandii* with proteomic and metabolomic methods.

Journal of Hazardous Materials 291 (2015) 52–64
http://dx.doi.org/10.1016/j.jhazmat.2015.02.063

Rafał Szewczyk, Adrian Soboń, Mirosława Słaba, Jerzy Długoński*

*Department of Biotechnology and Industrial Microbiology, Institute of Microbiology, Biotechnology and Immunology, Faculty of Biology and Environmental Protection, University of Łódź, Banacha 12/16, 90-237 Łódź, Poland, tel. +4842 635 44 65, Fax. +4842 665 58 18, jdlugo@biol.uni.lodz.pl

Abstract

Alachlor is a herbicide that is widely used worldwide to protect plant crops against broadleaf weeds and annual grasses. However, due to its endocrine-disrupting activity, its application has been banned in the European Union. As described in our earlier work, *Paecilomyces marquandii* is a microscopic fungus capable of alachlor removal by *N*-acetyl oxidation. Our current work employs proteomics and metabolomics to gain a better understanding of alachlor biodegradation by the microscopic fungus *P. marquandii*. The data revealed that the addition of alachlor reduced culture growth and glucose consumption rate. At the same time, the rates of glycolysis and the tricarboxylic acid (TCA) cycle increased during the initial stage of growth, and there was a shift toward the formation of supplementary materials (UDP-glucose/galactose) and reactive oxygen species (ROS) scavengers (ascorbate). Proteomic analysis revealed that the xenobiotic presence resulted in a strong upregulation of enzymes related to energy, sugar metabolism and ROS production. However, the unique overexpression of cyanide hydratase in alachlor-containing cultures may implicate this enzyme as the key protein involved in the alachlor biodegradation pathway. The characterization of *P. marquandii*-mediated alachlor removal in terms of cell structure and function resulted in a deeper insight into microorganism strategy toward xenobiotic biodegradation.

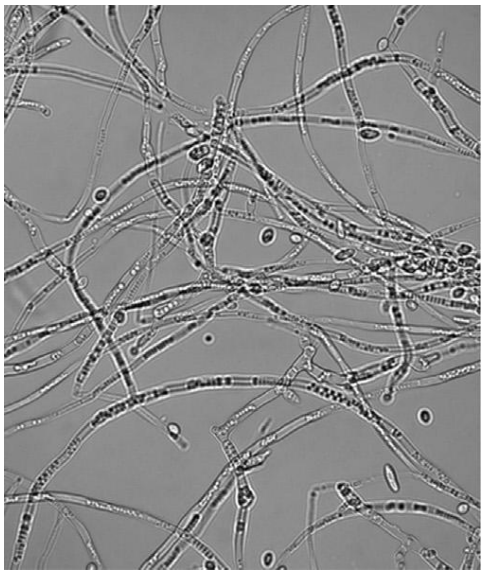

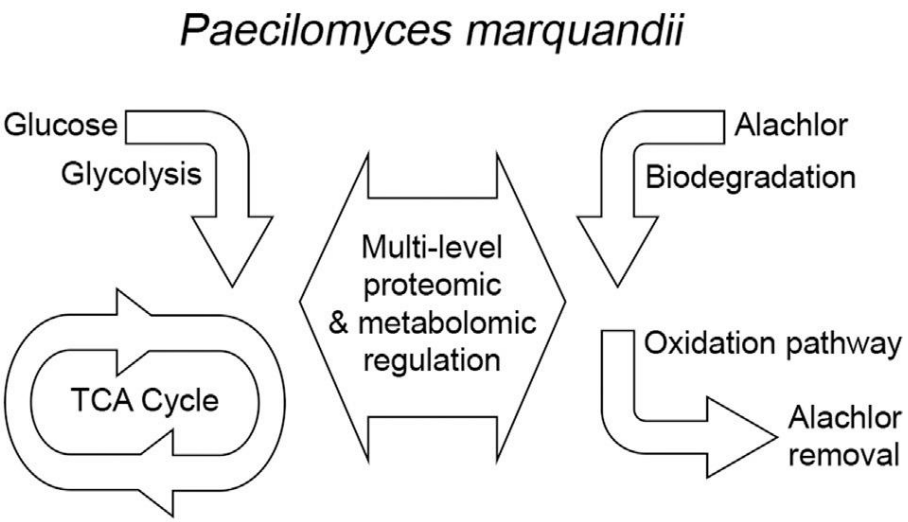

Keywords: fungi, alachlor, biodegradation, proteomics, metabolomics

1. Introduction

Alachlor is a pre-emergent chloroacetanilide herbicide that is widely used in world agriculture to protect plant crops (mainly corn) against broadleaf weeds and annual grasses. It is a selective systemic pesticide that interrupts both protein production and the synthesis of long-chain fatty acids in target plants [1,2]. Due to documented endocrine-disrupting activity, alachlor application has banned in the European Union. The risk to animal and human health is amplified by the high water solubility of alachlor (242 mg/L) and the resultant increased environmental mobility. Alachlor and its metabolites have been detected in soil, water and various biological samples [3]. Some of these intermediates are toxic or mutagenic e.g., 2,6-diethylaniline (DEA) [4,5].
Microbial degradation, or rather transformation, plays a pivotal role in the rate of alachlor elimination from the environment [6-8]. There are many studies concerning the both the characterization of selected microbial consortium or microorganisms in pure culture capable of degrading alachlor and the identification of byproducts, but little is known about the molecular mechanisms of conversions.
Proteomics and metabolomics are modern and convenient tools, which have been successfully applied to gain a better understanding of the biodegradation mechanisms in different types of organisms e.g., bacterial biodegradation of insecticide *N*-methylcarbamate by *Burkholderia* sp. C3 [9] or phenanthrene by *Sinorhizobium* sp. C4 [10]; fungal degradation of nonylphenol by *Metarhizium robertsii* [11]; *Mucor plumbeus* response to pentachlorophenol [12]; or benzoic acid removal by *Phanerochaete chrysosporium* [13]. Proteomic analysis has also been successfully applied to explore the plant phytoremediation mechanism of pyrene by *Scirpus triqueter* [14] or in the study of algae *Anabaena* sp. adaptations under butachlor pesticide action [15].
In our earlier work, *N*-acetyl oxidation was documented as the primary route of alachlor transformation by the microscopic filamentous fungus *P. marquandii* IM 6003. The possible metabolic pathway was also formulated [16]. In the present study, we elucidated the proteomic background of alachlor biodegradation as well as the changes in the primary sugar metabolism of fungus exposed to herbicide. To our knowledge, this is the first study on alachlor that employs microbial proteome expression in conjunction with multi-compound sugar metabolism research.

2. Materials and methods

2.1. Microorganism and culture conditions

Paecilomyces marquandii (S. Hughes, 1951), basionym: *Verticillium marquandii* (Massee, 1898), an alachlor-degrading filamentous fungus [16] from the collection of the Department of Industrial Microbiology and Biotechnology, University of Lodz (identification number: IM 6003) was examined in this work. This strain was selected from post-flotation dumps of non-ferrous metal works (Silesia, Poland) that were strongly polluted with heavy metals [17].
Applied culture conditions were the same as described previously [16].

2.2. Chemicals

Ethyl acetate and the ethanol needed for sample extractions and the high purity solvents used during sample preparation for LC-MS/MS analysis were purchased from Avantor (Poland). Alachlor, PESTANAL®, analytical standard (99.2%) and glucose standard were purchased from Sigma–Aldrich (Germany). All other chemicals and ingredients used in LC-MS/MS analysis, protein sample preparation and MALDI-TOF/TOF analysis were of high purity grade and obtained from Sigma-Aldrich (Germany), Serva (Germany), GE-Healthcare (Germany), Avantor (Poland), Promega (USA) or AB Sciex (USA).

2.3. Alachlor sample preparation

Following separation by filtration on Whatman 1 (Sigma, Germany), the mycelium was homogenized and extracted with ethyl acetate according to the procedures described previously [16].

2.4. Glucose metabolism sample preparation

Sample preparation was modified from a procedure developed by Wei et al. [18]. The filtration-separated mycelium was washed with water and weighed. The mycelium was then divided into 3 portions of 100 mg each and placed into 2-ml Eppendorf tubes containing 1 ml of cold water. Sections were then homogenized with a glass matrix (diameter 1 mm, 4°C) on FastPrep24 (MP Biomedicals, USA) three times for 30 s, with a velocity of 4 m s^{-1} and a 2 min brake for sample cooling on ice. The samples were then centrifuged at 4000 g, 4°C for 10 min. 100 µl of supernatant was transferred to separate 1.5-ml Eppendorf tubes containing 900 µl of 0.1% formic acid in ethanol and vortexed for 2-3 min. The samples were then incubated for 2 h, -20°C and centrifuged at 14000 g, 4°C for 20 min. The supernatant was transferred to a new 1.5-ml Eppendorf tube, evaporated until dry at 30°C under a vacuum and stored at -20°C for future analysis. Frozen samples were thawed at 4°C for 30 min followed by 15 min at room temperature, resuspension in 1 ml of water:acetonitrile (ACN) 98:2 (v/v), sonication and vortexing for 2 min and incubation for 60 min in 4°C. Finally, the samples were transferred to a 96-well plate for LC-MS/MS analysis.

2.5. LC–MS/MS qualitative and quantitative trend analysis and screening

The qualitative and quantitative LC–MS/MS analysis of alachlor biodegradation and glucose concentration was conducted with Agilent 1200 HPLC, coupled with AB Sciex 3200 QTRAP mass spectrometer according to methods developed previously [16,19]. A trend analysis of the alachlor metabolites was performed on the basis of precursor ion 162.1 m/z-extracted ion chromatograms, covering a scan range of 160 to 320 m/z [16].
The LC-MS/MS screening method applied for the glucose metabolism investigation was based on a multi-method developed by Wei et al. [18]. An AB Sciex 4500 QTRAP mass spectrometer (AB Sciex, USA), coupled with an Eksigent microLC 200 System (Eksigent, USA) were employed for analysis. Chromatography separation was conducted on an Eksigent C18-AQ (0.5 mm x 150 mm x 3 µm, 120 Å) column: temperature 35°C, injection volume 5 µl on the column. The eluent consisted of 2 mM of ammonium formate and 0.1% of formic acid in water (A) and ACN (B). The gradient used had a constant flow of 50 µl $min^{-1}$with 0.5 min of preflush conditioning, followed by 0.1 min in which98% of eluent A was used and then a decrease to 2% of eluent A for minutes 2.5-3.4. Initial conditions were restored from 3.5-4.0 min. The MS/MS detection was made in negative and positive ionization in multiple reaction-monitoring (MRM) mode. The optimized microESI ions source parameters were as follows: CUR: 25; IS: -4500 V; TEMP: 300°C; GS1: 30; GS2:30 and ihe:ON. Compound-dependent MRM parameters are presented in table S-1.

2.6. PCA analysis

Principle Component Analysis (PCA) was prepared with the MarkerView™ software (AB Sciex, USA) on MRM data (chromatography peak areas) from microLC-MS/MS analysis, with retention time locking in. After data set normalization against maximum and minimum values within the data set, the Pareto algorithm was applied for PCA calculation. Excel 2007 (Microsoft Corporation, USA) was used to report PCA loadings in the form of a heat map.

2.7. Protein extraction

Proteins from the mycelium were extracted with the use of mechanical homogenization on FastPrep24 (MP Biomedicals, USA) with glass beads (1-mm diameter), followed by TCA precipitation as described previously [11].

2.8. 2-D electrophoresis

Total protein content was measured using the Bradford method, with BSA (Sigma, Germany) as the protein standard. 2-D electrophoresis was conducted according to the procedure described previously [11] with modifications. Mycelial protein samples (500 µg) were loaded in 13 cm nonlinear IPG strips, pH 3-11 (GE Healthcare, Germany). Isoelectric focusing (IEF) was performed as follows: 60 V for 1 h, 120 V for 30 min, 150, 300 and 600 V (each for 1 h), 1500 V for 20 h, 1800, 2100, 2400 and 2700 V (each for 30 min), 3000 V for 44 h, 3300, 3600, 3900, 4100, 4400, 4700 and finally 5000 V (each for 1 h). The second dimension was performed using a 12% running gel with a stacking gel on the top. The separation was run at 100 V for the stacking gel and 220 V for the running gel (Hoefer, USA). A molecular mass standard covering the range of 6.5-200 kDa (Sigma, Germany) was used. Gels were stained with Coomassie blue. Comparative and statistical analysis of the gel triplicates was performed using Image Master 2D Platinum 7 software (GE Healthcare, Germany) and included automatic alignment of the gels, spot detection and measurement, background subtraction and subsequent normalization. After manual correction of mismatches within the data, spots with a p-value < 0.05 (and volume > 0.5) were considered to be significant.

2.9. Protein digestion

Protein digestion with trypsin was performed according to the procedure described previously [11].

2.10. MALDI-TOF/TOF analysis

AB Sciex 5800 TOF/TOF system (AB Sciex, USA) was used for data acquisition. Samples were placed on the MALDI plate twice, to cover the selection of the 25 strongest precursors for MS/MS analysis. The TOF MS analysis was conducted in the mass range of 800-4000 Da, 2400 V/400Hz laser relative energy, 2000 shots per sample and with the precursor selection order set from strongest to weakest. The instrument was externally calibrated in TOF MS mode with a peptide mixture (AB Sciex, USA) covering the tested mass range. The TOF/TOF MS/MS analysis was conducted in the mass range from 10-4000 Da, 3300 V/400Hz relative laser power, CID gas (air) at a pressure of ca $5x10^{-7}$ and up to 4000 shots per precursor with a dynamic exit. The precursor selection was set from the weakest to strongest in this mode. The external calibration of MS/MS mode with the fragments of Glu-fibrinopeptide (AB Sciex, USA) (1570.677 m/z) was applied.

2.11. Protein homology identification and functional alignment

Protein Pilot v4.5 software (AB Sciex, USA),coupled with Mascot search engine v2.4 [20] was used for initial database searches. The data were searched against the NCBI non-redundant database (version 05.2014; total number of sequences 38 633 935),with the taxonomy filtering the set to fungi (total number of fungi sequences 4 679 025). Mascot MS/MS ion searches were performed with trypsin chosen as the protein digesting enzyme, up to two missed cleavages were tolerated and the following variable modifications were applied: Acetyl (N-term), Carbamidomethyl (C), Deamidated (NQ), Gln to pyro-Glu (N-term Q), Glu to pyro-Glu (N-term E), Oxidation (M). Searches were conducted with a peptide mass tolerance of 50 ppm and a fragment ion mass tolerance of 0.3 Da.
Proteins identified and unidentified by MASCOT searches were further processed using a BLAST [21,22] search against the NCBI non-redundant protein sequences database (total number of sequences 38 633 935), with the use of the DELTA-BLAST algorithm (Domain Enhanced Lookup Time Accelerated BLAST) to confirm or define the probable function of the protein. The data for the BLAST searches derived from either Mascot results or, in the case of proteins unidentifiable by Mascot, were built on the basis of the set of single spot peptide sequences, manually evaluated with

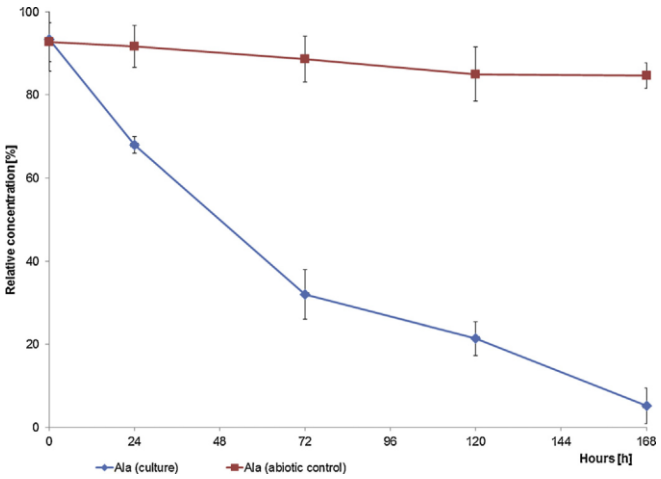

Fig. 1. Alachlor (50 mg L−1) biodegradation by *Paecilomyces marquandii* on Sabouraud medium *3.1. Alachlor biodegradation*

the use Data Explorer (AB Sciex, USA) and PeakView software with a Biotools plugin (AB Sciex, USA).

3. Results and discussion

As was shown previously [16], the tested strain is capable of efficient alachlor removal at the concentration of 50 mg L^{-1}. The degradation pathway included 10 metabolites formed by dechlorination and oxidation reactions of 2-chloro-N-(methoxymethyl)acetamide substituent. In the current work, we did not find any new metabolites using the applied LC-MS/MS method, and we therefore focused on the repeatability of alachlor removal as well as the repeatability of the trend analysis of alachlor derivatives. Analysis of replicates indicated that, in the case of alachlor removal, the standard deviation (SD) ranged from 2%-11%, while the trend analysis SDs were in the range of 6%-22%. The results demonstrated that the biodegradation course is reproducible in applied culture conditions, and the biodegradation curves are very similar to the ones published previously [16]. According to the data obtained from separate homogenized mycelium and culture medium extractions, removal of the xenobiotic takes place inside the cells of the tested strain. Alachlor removal and metabolite formation curves were used to determine the best time periods for intracellular proteome expression studies. Alachlor removal starts immediately; after the first 72 h, only 32% of alachlor is still present in the culture. After 168 h, 95% of the substrate is removed (Fig 1). On the other hand, the majority of the tested metabolites reached their relative concentration maximum after 120 h (Fig. 2). The data suggested that the 120 h cultures are best suited for comparative proteomic studies.

3.2. Glucose cometabolism

Metabolomics is a new system biology tool that has been employed in various scientific applications including medicinal chemistry, plant physiology and microbiology. However, the metabolomics of biodegradation is a completely new approach in this field. It comprehensively analyzes low molecular weight metabolites, including intermediates, and may include numerous primary and secondary metabolites [23].

Generating growth curves is essential for the metabolomic research of microbial cultures. The dry weight curves (Fig. 3) revealed that intensive growth in control cultures lasted until 96 h, whereas in alachlor-containing cultures, this phase ends after 120 h. Maximum growth is reached in both cultures after 144 h of culturing. However, the growth of alachlor-containing cultures is inhibited and reached 9.75 g L^{-1} in comparison to control cultures, where 11.51 g L^{-1} of dry weight was measured.

Glucose uptake reflects the growth potential of a strain under the tested conditions. A rapid decrease in concentration was observed in the cultures during the first 72 h of the experiment, but, as is demonstrated in Fig. 4, substrate depletion occurs more rapidly in the control cultures, where after 72 h, 7.33% of the glucose remained while in the alachlor-containing cultures, 20% of the glucose was detected. After 168 h in culture, glucose was completely absent from the control cultures, which was in contrast with xenobiotic-supplemented cultures, which still contained 5.15% of the substrate.

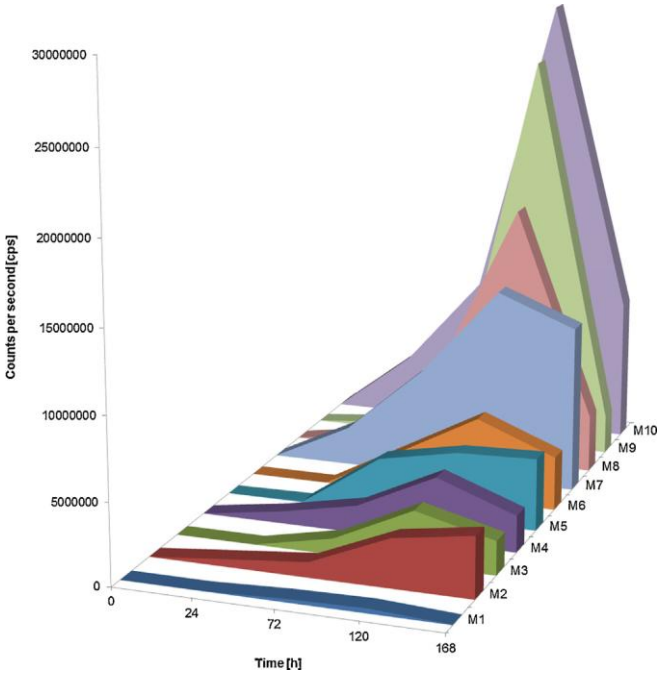

Fig. 2. Trend analysis of the identified metabolites duringalachlor (50 mg L−1) biodegradation by Paecilomyces marquandiion Sabouraud medium. Abbreviations means: M1 – N-[2-ethyl-6-(2-hydroxyethyl)phenyl]-N-(methoxymethyl)acetamide; M2– 2,6-diethyl-N-methylaniline; M3 – N-(2,6-diethylphenyl)-N-[(dihydroxymethoxy)methyl]-2-hydroxy-2-methoxyacetamide; M4 –N-(2,6-diethylphenyl)-2,2-dihydroxy-N-[(hydroxymethoxy)methyl]acetamide;M5 – N-(2,6-diethylphenyl)-2,2-dihydroxy-N-(methoxymethyl)acetamide; M6– (Z)-1-[(2,6-diethylphenyl)(methoxymethyl)amino]ethene-1,2-diol; M7 –N-(2,6-diethylphenyl)-2-hydroxy-N-(methoxymethyl)acetamide; M8 – N-(2,6-diethylphenyl)-N-[(dihydroxymethoxy)methyl]-2-methoxyacetamide; M9 –{(2,6-diethylphenyl)[(hydroxymethoxy)methyl]amino}(oxo)acetic acid; M10 –N-(2,6-diethylphenyl)-N-(methoxymethyl) acetamide.

Further insight into carbon source usage in the presence of the xenobiotic, was achieved by focusing on sugar metabolism. Therefore, this research primarily focused on glucose (glycolysis, TCA cycle) or glucose metabolism-related compounds, and it included 32 compounds analyzed in MRM mode on a microLC-MS/MS instrument. The applied LC-MS/MS method and sample preparation procedure was developed on the basis of a multi-method developed by Wei et al. [18] and modified for use with mycelia material extraction and analysis. The LC-MS/MS data from the control (c) and alachlor-containing (ala) cultures were subjected to principal component analysis (PCA) [24] with the use MarkerView software (AB Sciex, USA). The major differences occurred during the first 24 h of culture, as is presented in Fig.5, where samples 0 h and ala 24 are located on the PCA chart at the longest distances between both each other and the rest of the samples. The location of the samples on the chart is most affected by the high amounts of methylmalonate/succinate and UDP-glucose (samples ala 24), malate and aconitate (samples 0 h) and citrate (the rest of the samples) (Fig.5). Notable variation is also observed within the other samples, and sample groups c 24, ala 72, ala 120 & ala 168 and c 120 & c 168 tend to formulate clusters in different locations as compared to each other. To examine all data, PCA loadings for each analyte (peak areas) were averaged and recalculated to percentage values (100% is the highest loading for the analyte). The data are presented in Table 1, where the heat map and the simple chart scoring were applied to facilitate data evaluation. The data revealed a significant increase in the relative concentrations reaching the maximum or a high level of the selected compounds after 24 h of culturing in alachlor-containing cultures, especially hexose mono- and diphosphates, glycerol/glycerate group and end products of the TCA cycle (succinate, fumarate, malate, oxaloacetate). Similar behavior was observed for Acetyl-CoA. However, the citrate concentration was lower after 24 h in alachlor-containing cultures in comparison to control samples. On the other hand, citrate concentrations in both cultures were similar in all other tested time points. The maximum relative concentration in ala 24 samples was also observed for UDP-glucose/galactose, which is significant

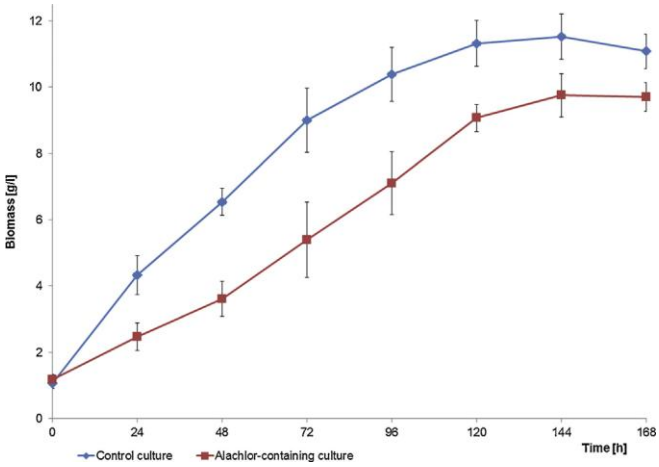

Fig. 3. Dry weight of the alachlor-containing (50 mg L−1) and control cultures of *Paecilomyces marquandii* on Sabouraud medium.

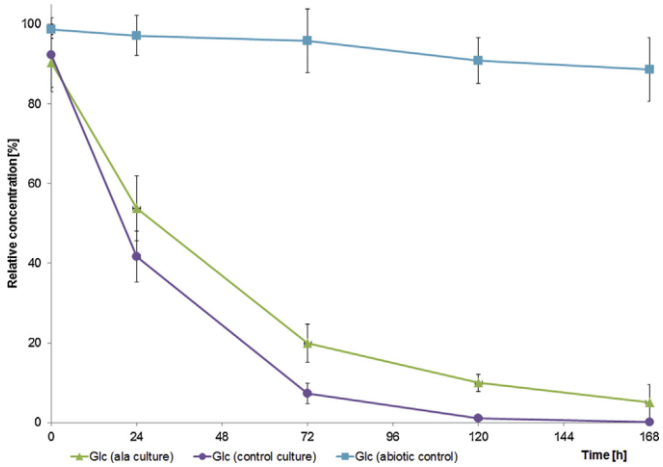

Fig. 4. Glucose consumption on alachlor-containing (50 mg L−1) and control cul-tures of *Paecilomyces marquandii* on Sabouraud medium.

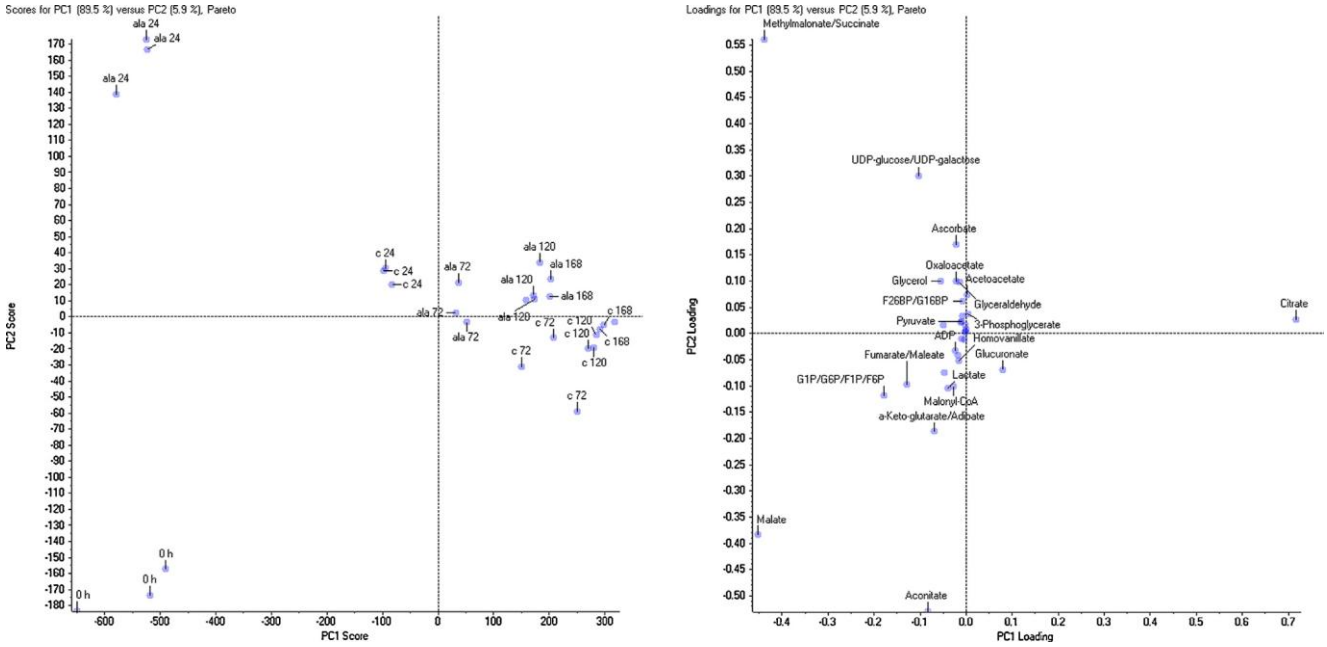

Fig. 5. PCA of the mycelial glucose metabolism on alachlor-containing (50 mg L−1) and control cultures on Sabouraud medium. On the left – PC1 against PC2 loadings chart;on the right – PC1 against PC2 scores chart.

Table 1. Relative concentration of the monitored compounds during alachlor (50 mg L−1) biodegradation by *Paecilomyces marquandii* on Sabouraud medium.

	Control culture					Alachlor containing culture				
Compound Name	0h	24h	72h	120h	168h	0h	24h	72h	120h	168h
3-Phosphoglycerate	34.0	63.9	26.6	30.4	40.1	24.8	83.2	100.0	79.3	38.7
Acetoacetate	35.1	100.0	74.2	63.7	56.0	44.6	86.8	54.5	64.8	96.2
Acetyl-CoA	100.0	25.8	18.5	9.3	10.1	92.4	72.2	8.2	0.0	0.0
Aconitate	100.0	43.2	45.1	38.4	36.1	86.6	26.3	55.7	22.2	19.5
ADP	100.0	41.0	20.7	5.7	4.2	86.5	50.2	23.4	8.9	10.2
a-Keto-glutarate/Adipate	100.0	40.6	25.6	20.2	19.6	86.9	37.0	24.3	27.4	25.7
AMP	100.0	9.2	3.0	2.1	3.0	96.0	32.6	4.2	2.9	2.3
Ascorbate	17.6	14.5	24.2	15.7	35.2	12.3	100.0	74.0	39.2	31.6
ATP	56.8	41.6	98.5	73.7	62.9	50.2	100.0	53.5	39.0	38.1
Citrate	61.9	85.0	96.1	99.0	100.0	68.4	67.6	89.8	95.2	95.7
F26BP/G16BP	5.5	42.5	21.8	10.1	33.3	7.0	100.0	71.3	21.7	18.6
Fumarate/Maleate	100.0	39.1	19.0	13.0	7.2	74.9	61.2	26.2	22.3	21.0
G1P/G6P/F1P/F6P	100.0	5.9	3.4	0.8	1.4	81.4	75.1	7.3	0.7	0.4
Glucuronate	48.4	62.4	89.7	100.0	98.1	58.6	47.6	84.3	79.0	74.3
Glyceraldehyde	17.1	41.9	32.0	23.8	24.0	18.7	100.0	35.7	38.4	20.1
Glycerate-2-P	16.9	27.9	6.5	9.7	13.1	19.7	100.0	27.0	43.2	24.7
Glycerol	54.7	18.2	13.2	11.3	13.4	39.4	100.0	9.0	10.2	12.8
Glycerol-3-P	80.2	11.1	3.8	3.9	3.5	68.5	100.0	3.9	3.8	1.1
Homovanillate	100.0	26.5	23.7	42.2	33.9	95.7	46.0	12.6	13.1	25.6
Lactate	100.0	25.8	77.2	57.1	19.8	89.7	35.7	17.2	17.4	44.8
Malate	100.0	37.4	14.2	8.8	5.6	88.4	74.0	23.7	17.8	18.8
Malonate	80.1	38.3	56.2	39.2	42.9	100.0	66.3	53.8	54.9	30.7
Malonyl-CoA	100.0	19.8	9.2	3.6	3.5	82.7	13.3	8.3	4.6	6.2
Methylmalonate/Succinate	71.9	51.8	14.7	10.7	8.5	60.7	100.0	39.0	21.5	20.1
Mevalonate	100.0	62.5	55.7	46.2	61.2	98.4	59.3	50.4	67.4	63.3
Oxalate	91.9	52.8	100.0	45.5	69.2	93.0	96.8	69.1	86.9	49.9
Oxaloacetate	60.7	40.1	50.0	51.4	71.9	63.6	100.0	61.7	61.7	54.3
PEP	100.0	29.4	33.6	9.9	28.6	93.5	30.0	22.3	20.8	20.5
Propionate	90.6	100.0	47.2	40.6	54.1	87.5	82.4	43.4	52.3	62.8
Pyruvate	56.5	100.0	68.7	39.4	23.1	46.9	76.9	76.3	50.4	20.4
UDP-glucose/UDP-galactose	34.8	29.1	4.4	9.8	13.1	27.8	100.0	9.8	14.2	12.5
UDP-glucuronate	51.3	49.9	66.2	42.2	100.0	46.8	83.3	41.2	70.9	96.9

Legend: 20.0 40.0 60.0 80.0 100.0

because in all other samples, the relative concentration was lower by 70-90%. Interestingly, ascorbate and 3-phosphoglycerate concentrations significantly increased in ala 24, ala 72 and ala 120 samples in comparison to the other samples.

Metabolomic analyses of the white-rot fungus *P. chrysosporium* exposed to benzoic acid (BA) included various compounds such as glycolysis intermediates, TCA cycle intermediates, amino acids and lipids [13] determined by the untargeted GC-MS method. It was found that to effectively metabolize BA, fungal regulation of the TCA cycle and mannitol cycles as well as the regulation and utilization of trehalose as a storage sugar were observed. In the case of TCA cycle metabolites, the majority of the compound concentrations decreased in the presence of BA. Similarly, the few glycolysis intermediates (ex. glucose, glucose-6-phosphate, glycerol-3-phosphate) also decreased in concentration or stayed at the same level, contrary to the results obtained in this work. A comprehensive metabolomic study on bacterium *Sinorhizobium* sp. C4 during the degradation of phenanthrene [10] also included numerous compounds measured using the untargeted GC-MS method. Among the other compounds, the differential study also included organic acids, glycolysis and TCA cycle metabolites. In general, a higher accumulation of some intermediates from glycolysis (e.g., 2-phosphoglycerate), the TCA cycle (e.g., oxalate) and others (2-hydroxyglutarate, malonate and 3-hydroxyisovalerate) were found in the phenanthrene-supplemented culture, with a parallel reduction in the level of other metabolites in the same pathway (e.g., 3-phosphoglycerate, malate and α-ketoglutarate).

In summary, the addition of alachlor drives the source of carbon metabolism towards higher and more efficient consumption during

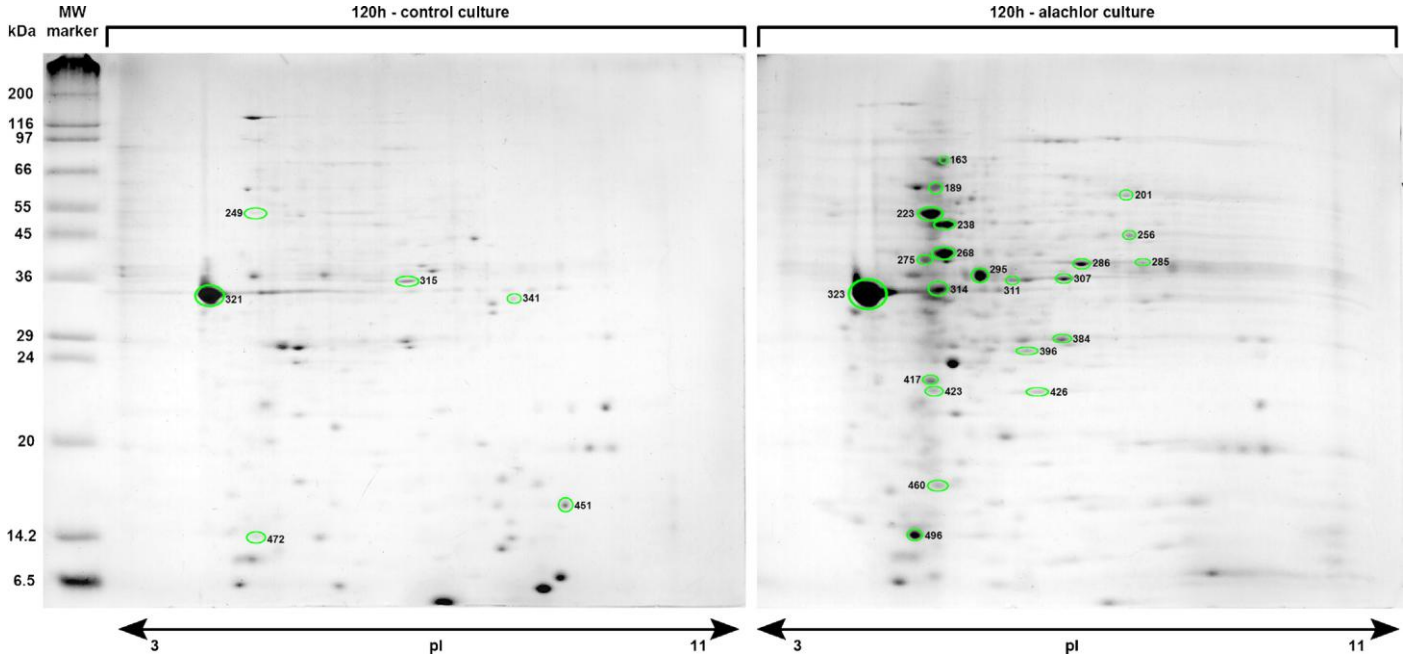

Fig. 6. 2-D electrophoresis gels after 120 h of Paecilomyces marquandii culture. Marked spots were analyzed and identified by MALDI–TOF/TOF sequencing followed bydatabase searches.

the initial stage of growth (increased glycolysis and TCA cycle rate), but it also changed the glucose utilization to form polysaccharides, supplementary materials, lipopolysaccharides and glycosphingolipids (UDP-glucose/galactose) and ascorbate, which is known to act as a powerful reducing agent, capable of rapidly scavenging a number of reactive oxygen species that may be formed in this case during alachlor biodegradation. The more efficient consumption of glucose, accompanied by the slowdown of growth curves, may be a result of the high-stress conditions in alachlor-containing cultures. However the toxic influence of the xenobiotic may directly affect glucose consumption, growth and the concentration of other compounds involved in intracellular metabolism.

3.3. Proteomic studies

Despite the prevalence of these organisms in the various fields of biotechnology, industry, environmental protection and medicine [11,13,25-28], proteomic studies of filamentous fungi are a new trend in the research. To our knowledge, the proteomics (especially intracellular proteomics) of the fungal biodegradation is represented by a very small number of research papers. This paucity of proteomic studies is likely due to the challenge of protein extraction, as this group of microorganisms secrete proteases, display polarized growth, have heavily clustered microtubules organelles and generally possess thick, compact cell walls [29]. The method of protein extraction we developed for *M. robertsii* [11] has been successfully applied to our current work for the extraction of intracellular proteins from *P. marquandii*.

Our data revealed that at 120 h, the cultures are best suited for the comparative proteomics of alachlor biodegradation by *P. marquandii*. Extraction of the intracellular proteome was followed by 2-D electrophoresis separation, revealing the presence of 247 and 265 protein spots in control and alachlor containing samples, respectively (Fig. 6). The gel analysis conducted with ImageMaster 2D Platinum software resulted in the matching of 93 spots and allowed for a comparison of relative expression between the samples on the basis of the percentage of the spot volume quantitation done after total volume normalization within the gels. In the case of unmatched spots, the relative volume of 0.5% or higher was used as a criterion for the spots excised. Within the matched spots, the fold change analysis was performed, and spots that were characterized by a 2-fold or higher change in up- or down regulation were subjected to spots excision. The applied criteria resulted in the selection of 58 proteins from control cultures and 42 proteins from alachlor-containing cultures for trypsin digestion, followed by MALDI-TOF/TOF sequencing.

The proteomic background of gossypol (a derivative of naphthalene) biodegradation by *Aspergillus niger* AN-1 was investigated by Yang et al. [30] with glucose or gossypol acting as a sole source of carbon in cultures. 478 spots were detected on the glucose gel, whereas 592 spots were detected on the gossypol gel. An average of 293 protein spots were matched on both gels. Through 2-DE analysis, 51 protein spots, which may be related to the biodegradation of gossypol, were differentially expressed between the two carbon sources. A total of 20 spots of interest were identified using MALDI-TOF MS, where 4 proteins were related to energy metabolism, while 14 proteins were identified as either unnamed or hypothetical proteins from *A. niger*. Whole proteome analysis of PCP biodegradation by *M. plumbeus* revealed the presence of over 700 protein spots in control and PCP-treated cultures [12]. On the basis of the proteins identified, it was demonstrated that exposure to PCP leads to upregulation of several proteins involved in defense mechanisms against stress (e.g., HSP70, cytochrome c peroxidase and thiamine biosynthetic enzymes). However, as the authors stated, none of the mycelial or extracellular proteins found were involved in the PCP biodegradation pathway. This is with the exception of the ADH mycelial protein, which is thought to play an important role in the last steps of PCP degradation. The key step of the biodegradation of 4-*n*-nonylphenol (4-*n*-NP) by *M. robertsii* [11] took place after 24 h of culturing. 2-DE analysis showed the expression of 205 and 208 protein spots in the control and 4-*n*-NP supplemented cultures, respectively. 88 spots matched in both gels and were differentially expressed in the cultures. However, the differences were not significant (below 1-fold). The main differences included 14 protein spots present only in control samples and 19 protein spots present only in xenobiotic containing cultures. The identification of selected proteins based on the MALDI-TOF/TOF sequencing of tryptic digests helped explain the proteomic background of 4-*n*-NP removal, which involved oxidation-reduction systems, ROS defense systems, the TCA cycle and energy-related systems.

The proteins identified in *P. marquandii* cultures are presented in the Table 2 and 3, and the full set of the database searches are shown in the tables S-2 and S-3. The homology (Mascot searches) and functional alignments (BLAST searches with the delta-blast algorithm) within the 100 tested protein spots allowed for the identification and/or functional assignment of 28 protein spots, although the tested strain is not sequenced. These included 7 out of 58 selected protein spots in control cultures and 21 out of 42 selected protein spots in the alachlor-containing cultures. In both cultures, the dominant matched spots 321 and 323 have more than one hit in the database including stress protein DDR48 (control culture), N-acetylmuramoyl-L-alanine (ala culture), amidase transcription termination factor Rho and mold-specific protein (both cultures).The possibility cannot be excluded that within a spot of that size more than one protein is located, but regarding further database hits (data not shown) the structural mold-specific protein is the major component of the spot. Both cultures are characterized by the presence of energy-related (ATP synthase) and sugars metabolism enzymes (kinases, transaldolases, reductases, dehydrogenases, mutases and isomerases). However in the alachlor-containing

Table 2. Summary of Mascot and BLAST search results after 120 h of the Paecilomyces marquandii control culture. Mascot algorithm matching – protein scores greater than 73 aresignificant ($p < 0.05$). Delta-BLAST algorithm – the lower the E-value (closer to zero), the more significant is the match.

Spot ID.	Mascot search result							DELTA-BLAST Results
	Best Protein Accession	Mass [Da]	Calc. pI	Peptides Matched	Seq. Cov.	Score	Best Protein Description	
249/247	gi|358398002	54863	5.47	31	50%	194	ATP synthase beta chain mitochondrial precursor [Trichoderma atroviride IMI206040]	[cd01133] F1- ATP synthase beta subunit, nucleotide-binding domain; E=0e+00 [cl08258] ATP synthase alpha/beta chain, C-terminal domain; E=2.38e-33 [cl18399] ATP synthase alpha/beta family, beta-barrel domain; E=5.22e-19 [PRK09280] F0-F1 ATP synthase subunit beta; Validated;E=0e+00
	gi|400595077	55284	5.26	29	45%	171	ATP synthase beta chain [Beauveria bassiana ARSEF2860]	
	gi|471567117	54831	5.46	25	38%	159	putative atp synthase beta mitochondrial precursor protein [Eutypalata UCREL1]	
314	gi|322697295	35337	6.49	30	51%	105	transaldolase [MetarhiziumacridumCQMa102]	[cd00957] transaldolases including both TalA and TalB; E=2.63e-176 [PTZ00411] transaldolase-like protein; Provisional; E=5.88e-152
	gi|322712191	34600	6.86	27	34%	105	transaldolase [MetarhiziumanisopliaeARSEF23]	
	gi|399165577	35653	5.64	20	29%	105	probable transaldolase [Clavicepspurpurea20.1]	
321	gi|240280489	33573	4.83	23	51%	246	stress protein DDR48 [Ajellomyces capsulatus H143]	[PRK12678] transcription termination factor Rho; Provisional; E=3.38e-04
	gi|154277766	32925	4.57	18	46%	237	hypothetical protein HCAG_05184 [Ajellomyces capsulatus NAm1]	
	gi|13591791	31617	4.95	17	40%	229	mold-specific protein MS95 [Ajellomyces capsulatus]	
341	gi|302892809	34444	6.14	18	33%	151	predicted protein [Nectria haematococca mpVI 77-13-4]	[cd01337] glyoxysomal and mitochondrial malate dehydrogenases; E=0e+00 [PLN00106] malate dehydrogenase; E=1.30e-143
	gi|322695422	34218	6.46	17	29%	151	malate dehydrogenase precursor [Metarhizium acridum CQMa 102]	
	gi|531862512	43794	9.21	20	30%	151	malate dehydrogenase [Ophiocordyceps sinensis CO18]	
364	gi|531866468	36308				68	outer mitochondrial membrane protein porin [Ophiocordyceps sinensis CO18]	[cd07306] voltage-dependent anion channel of the outer mitochondrial membrane; E=1.10e-86 [pfam01459] eukaryotic porin; E=1.14e-80
451	gi|70984978	16922	7.77	12	60%	265	nucleoside diphosphate kinase [Aspergillus fumigatus Af293]	[cd04413] nucleoside diphosphate kinase group I (NDPk_I)-like; E=5.04e-91 [pfam00334] nucleoside diphosphate kinase; E=5.36e-88
	gi|471560787	16736	7.77	11	41%	265	putative nucleoside diphosphate kinase protein [Eutypa lata UCREL1]	
	gi|30315965	16898	7.82	11	56%	263	RecName: Full=Nucleoside diphosphate kinase; Short=NDP kinase; AltName: Full=AnNDK; Short=NDK	
472	gi|340519078	12201	4.72	5	23%	103	predicted protein [TrichodermareeseiQM6a]	[DUF3759] protein of unknown function; E=1.93e-35

Table 3. Summary of Mascot and BLAST search results after 120 h of the Paecilomyces marquandii culture containing alachlor (50 mg L−1). Mascot algorithm matching – protein scores greater than 73 are significant ($p < 0.05$). Delta-BLAST algorithm – the lower the E-value (closer to zero), the more significant is the match.

Spot ID.	Mascot search results							DELTA-BLAST Results
	Best Protein Accession	Mass [Da]	Calc. pI	Peptides Matched	Seq. Cov.	Score	Best Protein Description	
160	gi|531865828	72449	5.7	32	32%	410	heat shock 70 kDa protein [Ophiocordyceps sinensis CO18]	[cd11733] nucleotide-binding domain of human HSPA9, Escherichia coli DnaK, and similar proteins; E=0e+00 [PRK00290] molecular chaperone DnaK; Provisional; E=0e+00
	gi|322701734	73112	5.68	40	41%	368	heat shock 70 kDa protein precursor [Metarhizium acridum CQMa 102]	
	gi|322706829	73386	5.68	37	40%	367	heat shock 70 kDa protein [Metarhizium anisopliae ARSEF 23]	
189	gi|322700211	62929	5.38	33	38%	155	phosphoglycerate mutase, 2,3-bisphosphoglycerate-independent [Metarhizium acridum CQMa 102]	[PRK05434]phosphoglyceromutase; Provisional; E=0e+00 [Superfamily] cl17463, BPG-independent PGAM N-terminus (iPGM_N)
	gi|322708166	63375	5.49	33	39%	155	2,3-bisphosphoglycerate-independent phosphoglycerate mutase (iPGM) [Metarhizium anisopliae ARSEF 23]	
	gi|346326764	58747	5.25	26	27%	125	phosphoglycerate mutase, 2,3-bisphosphoglycerate-independent [Cordyceps militaris CM01]	
201	gi|358399574	56475	6.26	25	28%	153	peroxisomal catalase [Trichoderma atroviride IMI 206040]	[cd08157] fungal catalases similar to yeast catalases A and T; E=0e+00 [COG0753] catalase; E=0e+00
	gi|6014693	57211	6.79	21	29%	123	catalase isozyme P [Ajellomyces capsulatus]	
	gi|24528587	56849	6.5	14	21%	123	catalase [Paracoccidioides brasiliensis]	
223	gi|531866883	55138	5.33	33	57%	146	ATP synthase beta chain [Ophiocordyceps sinensis CO18]	[cd01133], F1 ATP synthase beta subunit, nucleotide-binding domain; E=0e+00 [Cdd:pfam00306] ATP synthase alpha/beta chain, C terminal domain; E=1.32e-31 [Cdd:pfam02874] ATP synthase alpha/beta family, beta-barrel domain; E=3.60e-19 [PRK09280] F0-F1 ATP synthase subunit beta; Validated; E=0e+00
	gi|399171671	55040	5.48	23	41%	129	H+-transporting ATP synthase beta chain [Claviceps purpurea 20.1]	
	gi|440638891	55382	5.46	28	41%	117	ATP synthase subunit beta, mitochondrial [Pseudogymnoascus destructans 20631-21]	
238/242	gi|399170765	47165	5.39	15	35%	288	probable enolase (2-phosphoglycerate dehydratase) [Claviceps purpurea 20.1]	[cd03313] enolase; E=0e+00 [PLN00191] enolase; E=0e+00
	gi|477534317	47183	5.23	12	30%	264	enolase [Colletotrichum orbiculare MAFF 240422]	
	gi|212537563	47395	5.39	13	30%	171	enolase/allergen Asp F 22 [Talaromyces marneffei ATCC 18224]	
256	gi|322696440	52422	8.43	29	29%	198	Phosphoglycerate kinase [Metarhizium acridum CQMa 102]	[cd00318] phosphoglycerate kinase (PGK);

	gi|322704254	44347	6.69	27	36%	198	Phosphoglycerate kinase [Metarhizium anisopliae ARSEF 23]	E=0e+00 [Superfamily] cl00198, phosphoglycerate kinase (PGK)
	gi|302886659	44613	5.43	21	38%	129	predicted protein [Nectria haematococca mpVI 77-13-4]	
268	gi|322702591	39769	5.53	20	34%	109	cyanide hydratase [Metarhizium anisopliae ARSEF 23]	[cd07564] nitrilases, cyanide hydratase (CH)s, and similar proteins (class 1 nitrilases); E=2.75e-119
	gi|88766405	39768	5.63	20	34%	109	cyanide hydratase [Metarhizium anisopliae]	
275	gi|346322842	42559				68	vacuolar protease A precursor [Cordyceps militaris CM01]	[cd05471] pepsin-like aspartic proteases; E=3.95e-97 [pfam00026] eukaryotic aspartyl protease; E=1.54e-119
285	gi|225559211	36835	8.26	16	28%	80	NADP-dependent glycerol dehydrogenase [Ajellomyces capsulatus G186AR]	[cd06660] aldo-keto reductases; E=7.51e-78
	gi|261204493	37322	6.28	15	30%	80	aldehyde reductase I [Ajellomyces dermatitidis SLH14081]	
	gi|239614213	37350	6.43	15	29%	80	aldehyde reductase I [Ajellomyces dermatitidis ER-3]	
286	gi|429862698	36234	6.25	33	55%	366	glyceraldehyde-3-phosphate dehydrogenase [Colletotrichum gloeosporioides Nara gc5]	[pfam02800] glyceraldehyde 3-phosphate dehydrogenase, C-terminal domain; E=7.93e-100 [pfam00044] glyceraldehyde 3-phosphate dehydrogenase, NAD binding domain; E=9.57e-80 [COG0057] glyceraldehyde-3-phosphate dehydrogenase/erythrose-4-phosphate dehydrogenase; E=0e+00
	gi|530477121	36248	6.25	31	55%	335	glyceraldehyde-3-phosphate dehydrogenase [Colletotrichum gloeosporioides Cg-14]	
	gi|477536372	36232	6.24	30	51%	333	glyceraldehyde-3-phosphate dehydrogenase [Colletotrichum orbiculare MAFF 240422]	
295	gi|302884358	39125	5.24	13	27%	139	fructose-bisphosphate aldolase [Nectria haematococca mpVI 77-13-4]	[PRK09197] fructose-bisphosphate aldolase; Provisional; E=0e+00 [Superfamily] cl17181, fructose/tagarose-bisphosphate aldolase class II
	gi|342871910	37275	5.24	10	21%	127 127	hypothetical protein FOXB_15150 [Fusarium oxysporum Fo5176]	
	gi|475673861	39633	5.44	10	20%		Fructose-bisphosphate aldolase [Fusarium oxysporum f. sp. cubense race 4]	
307	gi|322697295	35337	6.49	38	51%	207	transaldolase [Metarhizium acridum CQMa 102]	[cd00957] transaldolases including both TalA and TalB; E=2.63e-176 [PTZ00411] transaldolase-like protein; Provisional; E=5.88e-152
	gi|322712191	34600	6.86	35	44%	195	transaldolase [Metarhizium anisopliae ARSEF 23]	
	gi|531856223	35087	6.86	34	49%	194	Transaldolase [Ophiocordyceps sinensis CO18]	
311	gi|322697295	35337	6.49	30	39%	76	transaldolase [Metarhizium acridum CQMa 102]	[cd00957] transaldolases including both TalA and TalB; E=2.63e-176 [PTZ00411] transaldolase-like protein; Provisional; E=5.88e-152
	gi|322712191	34600	6.86	28	41%	76	transaldolase [Metarhizium anisopliae ARSEF 23]	
	gi|399165577	35653	5.64	23	29%	76	probable transaldolase [Claviceps purpurea 20.1]	
314	gi|67539148	30223	4.85	16	28%	161	hypothetical protein AN5744.2 [Aspergillus nidulans FGSC A4]	[cd11309] fungal 14-3-3 protein domain; E=2.80e-138 [Superfamily] cl02098, 14-3-3 domain
	gi|46108718	27506	4.94	14	22%	161	hypothetical protein FG01241.1 [Fusarium graminearum PH-1]	
	gi|70991439	30085	4.74	16	35%	161	14-3-3 family protein [Aspergillus fumigatus Af293]	
323/4	gi|302654183	20680	4.83	15	20%	202	conserved hypothetical protein [Trichophyton verrucosum HKI 0517]	[PRK12678] transcription termination factor Rho; Provisional; E=0.01 [PRK08581] N-acetylmuramoyl-L-alanine amidase; Validated; E=0.03
	gi|530473648	32195	4.45	20	47%	187	hypothetical protein CGLO_06169 [Colletotrichum gloeosporioides Cg-14]	
	gi|261196113	40526	6.85	32	46%	186	mold-specific protein [Ajellomyces dermatitidis SLH14081]	
384	gi|401888325	27630	7.64	15	40%	75	L-xylulose reductase [Trichosporon asahii var. asahii CBS 2479]	[cd05352] mannitol dehydrogenase (MDH)-like, classical (c) SDRs; E=1.03e-119 [PRK05557] 3-ketoacyl-(acyl-carrier-protein) reductase; Validated; E=1.81e-52
396	gi|346327419	26911	6.02	14	32%	139	triosephosphate isomerase [Cordyceps militaris CM01]	[cd00311] triosephosphate isomerase (TIM); E=8.40e-111
	gi|315042127	27047	5.59	12	30%	110	triosephosphate isomerase [Arthroderma gypseum CBS 118893]	
	gi|302672679	26429	6.1	6	10%	104	hypothetical protein SCHCODRAFT_71461 [Schizophyllum commune H4-8]	
423	gi|46124419	23107				72	RS7_NEUCR 40S ribosomal protein S7 [Fusarium graminearum PH-1]	[pfam01251] ribosomal protein S7e; E=5.11e-101
426	gi|322707797	24900				60	manganese superoxide dismutase [Metarhizium anisopliae ARSEF 23]	[pfam02777] iron/manganese superoxide dismutases, C-terminal domain; E=1.25e-50 (super family) cl02809; E=1.92e-33 [COG0605] superoxide dismutase; E=7.09e-90
460	gi|340518820	14822	10.12	16	48%	86	histone H2B [Trichoderma reesei QM6a]	[smart00427] histone H2B; E=4.30e-49 [Superfamily] cl00074, histone H4
	gi|358385634	14836	10.12	16	48%	86	hypothetical protein TRIVIDRAFT_92198 [Trichoderma virens Gv29-8]	
	gi|51701481	14789	10.16	14	42%	86	RecName: Full=Histone H2B	
496	gi|340519078	12201	4.72	7	23%	82	predicted protein [Trichoderma reesei QM6a]	[DUF3759] protein of unknown function; E=1.93e-35

cultures, significantly increased expression of this group of proteins, resulting in 11 enzymes identified in comparison to control samples where only 4 enzymes from this group were found. This result is in agreement with the glucose metabolism data wherein the alachlor-containing cultures exhibit slower growth and glucose uptake, leading to the differences in the metabolic pathways courses. The upregulation of the energy-related and sugars metabolism proteins during xenobiotics biodegradation seems to be a common effect of its presence in the culture [11,30]. The upregulation of reactive oxygen species (ROS) enzymes represented by the manganese superoxide dismutase and catalase was observed in alachlor-containing cultures. The production of ascorbate as well as results from our proteomic studies support the fact that during alachlor biodegradation, ROS are generated and both classes of compounds may act as a self-defense mechanism during xenobiotic removal. Similar upregulation of ROS enzymes was observed in cultures of *M. robertsii* exposed to 4-*n*-NP [11]. On the other hand, the ROS enzymes' oxidoreductase activity towards alachlor itself cannot be excluded as the enzymes expression may take place under other physiological and non-physiological conditions [31]. In addition, the typical stress response protein - heat shock 70 kDa protein, was upregulated only in alachlor-containing cultures as in the cultures of

M. plumbeus exposed to pentachlorophenol (PCP) [12]. An interesting result was obtained from alachlor-containing culture spot 268, identified as cyanide hydratase – a nitrilase (class 1 nitrilase or nitrile aminohydrolase), which is capable of hydrolyze nitriles (RCN) to ammonia and the corresponding carboxylic acid. Most nitrilases prefer aromatic nitriles, some prefer aryl acetonitriles and other aliphatic nitriles. The mechanism of alachlor biodegradation was explained in our previous work [16], illustrating that the pathway includes changes in the aliphatic substituent of alachlor, leading to the dechlorination and the formation of different oxidized forms (ex. carboxylic acids, ketones or alcohols) of both chains situated next to the C-N bond of 1-(2,6-diethylphenyl)methanamine substituent. Given the overexpression of this enzyme in cultures upon xenobiotic addition, it is likely that it is a key protein involved in the *P. marquandii*-mediated biodegradation process of alachlor.

4. Conclusion

The living cell is a huge biochemical manufacturer – our research focused on a specific process, but more detailed information on multilevel metabolic adaptations may provide a better understanding of any environmentally relevant organism, allowing us to enhance or modify a given process for specific purposes. To our knowledge, this is the first study combining proteomics and primary metabolomics to assess alachlor biodegradation by a fungal strain.

Our data indicate that the addition of alachlor reduced culture growth and glucose consumption rate. However, the carbon source metabolism increased (glycolysis and TCA cycle) during the initial stage of growth, and a shift towards the formation of supplementary materials (UDP-glucose/galactose) and ascorbate (powerful ROS scavenger) was observed. The proteomics of the process tested revealed that, in the presence of a strong xenobiotic, sugars, as well as energy, metabolism and ROS enzymes are upregulated. Additionally, the unique overexpression of cyanide hydratase in alachlor-containing cultures, which hydrolyze nitriles to ammonia and the corresponding carboxylic acid, may indicate that this enzyme is the most important in the process examined.

The characterization of alachlor removal by *P. marquandii*, including xenobiotic pathway research [16] and trend analysis, basic physiological measurements, combined with primary metabolite profiling and proteomics, resulted in deeper insight into a microorganism's approach towards xenobiotic biodegradation on various levels of cell structure and functionality.

Acknowledgments

This study was supported by the grant of the National Science Centre, Poland (Project No. UMO-2011/01/B/NZ9/02898).

References

[1] P. Böger, B. Matthes, J. Schmalfuß, Towards the primary target of chloroacetamides – new findings pave the way, Pest. Man. Sci. 56 (2000) 497-508.

[2] L.D. Sette, L.A. Mendonca Alves da Costa, A.J. Marsaioli, G.P. Manfio, Biodegradation of alachlor by streptomycetes, Appl. Microbiol. Biotechnol. 64 (2004) 712–717.

[3] L. Fava, P. Bottoni, A. Crobe, E. Funari, Leaching properties of some degradation products of alachlor and metolachlor, Chemosphere 41 (2000) 1503-1508.

[4] D.M. Tessier, J.M. Clark, Quantitative assessment of the mutagenic potential of environmental degradative products of alachlor, J. Agric. Food Chem. 43 (1995) 2504-2512.

[5] C.Z. Chen, C.T. Yan, P.V. Kumar, J.W. Huang, J.F. Jen, Determination of alachlorand its metabolite 2,6-diethylaniline in microbial culture medium using online microdialysis enriched sampling coupled to high performance liquid chromatography,J. Agric. Food Chem. 59 (2011) 8078–8085.

[6] W. Charles, D. Knappa, W. Grahama, G. Berardescoa, F. de Noyelles Jr, B.J. Cutakd, C.K. Larive, Nutrient level, microbial activity, and alachlor transformation inaerobic aquatic systems, Water Res. 37(2003) 4761–4769.

[7] A.E.M. Chirnside, W.F. Ritter, M. Radosevich, Biodegradation of aged residuesof atrazine and alachlor in a mix-load site soil. Soil Biol.Biochem. 41 (2009) 2484–2492.

[8] Munoz, W.C. Koskinen, L. Cox, M.J. Sadowsky, Biodegradation and mineralization of metolachlor and alachlor by *Candida xestobii*, J. Agric. Food Chem. 59 (2011) 619-627.

[9] J.-S. Seo, Y.-S. Keum, Q.X. Li, Metabolomic and proteomic insights into carbaryl catabolism by *Burkholderia* sp. C3 and degradation of ten *N*-methylcarbamates, Biodegradation 24 (2013) 795-811.

[10] Y.S. Keum, J.S. Seo, Q.X. Li, J.H. Kim, Comparative metabolomic analysis of *Sinorhizobium* sp. C4 during the degradation of phenanthrene, Appl. Microbiol. Biotechnol. 80 (2008) 863–872.

[11] R. Szewczyk, A. Soboń, S. Różalska, K. Dzitko, D. Waidelich, J. Długoński, Intracellular proteome expression during 4-*n*-nonylphenol biodegradation by the filamentous fungus *Metarhizium robertsii*, Int. Biodeterior. Biodegrad. 93 (2014) 44–53.

[12] M.B. Carvalho, I. Martins, J. Medeiros, S. Tavares, S. Planchon, J. Renaut, O. Núñez, H. Gallart-Ayala, M.T. Galceran, A. Hursthouse, C. Silva Pereira, The response of *Mucor plumbeus* to pentachlorophenol: a toxicoproteomics study, J. Proteomics 78 (2013) 159–171.

[13] F. Matsuzaki, M. Shimizu, H. Wariishi, 2008. Proteomic and metabolomic analyses of the White-Rot fungus *Phanerochaete chrysosporium* exposed to exogenous benzoic acid, J. Proteome Res. 7 (2008) 2342-2350.

[14] X. Zhang, X. Liu, W. Chai, J. Wei, Q. Wang, B. Li, H. Li, The use of proteomic analysis for exploring the phytoremediation mechanism of *Scirpus triqueter* to pyrene, J. Hazard. Mater. 260 (2013) 1001–1007.

[15] C. Agrawal, S. Sen, S. Singh, S. Rai, P.K. Singh, V.K. Singh, L.C. Rai, Comparative proteomics reveals association of early accumulated proteins in conferring butachlor tolerance in three N2-fixing *Anabaena* sp., J. Proteomics 96 (2014) 271-290.

[16] M. Słaba, R. Szewczyk, M.A. Piątek, J. Długoński, Alachlor oxidation by the filamentous fungus *Paecilomyces marquandii*, J. Hazard. Mater. 261 (2013) 443–450.

[17] M. Słaba, J. Długoński, Selective recovery of Zn^{2+} from waste slag from a metal-processing plant by microscopic fungus *Verticillium marquandii*, Biotechnol. Lett. 22 (2000) 1699–1704.

[18] R. Wei, G. Li, A.B. Seymour, High-throughput and multiplexed LC/MS/MRM method for targeted metabolomics, Anal. Chem. 82 (2010) 5527–5533.

[19] S. Różalska, R. Szewczyk, J. Długoński, Biodegradation of 4-*n*-nonylphenol by the non-ligninolytic filamentous fungus *Gliocephalotrichum simplex*: a proposalof a metabolic pathway, J. Hazard. Mater. 180 (2010) 323–331.

[20] D.N. Perkins, D.J. Pappin, D.M. Creasy, J.S. Cottrell, Probability-based protein identification by searching sequence databases using mass spectrometry data, Electrophoresis 20 (1999) 3551–3567.

[21] S.F. Altschul, W. Gish, W. Miller, E.W. Myers, D.J. Lipman, Basic local alignment search tool, J. Mol. Biol. 215 (1990) 403–410.

[22] Basic Local Alignment Search Tool, The National Center for Biotechnology Information, 2014 online at: http://blast.st-va.ncbi.nlm.nih.gov/Blast.cgi?PROGRAM=blastp&PAGE_TYPE=BlastSearch&LINK_LOC=blasthome

[23] D. Miura, H. Tanaka, H. Wariishi, Metabolomic differential display analysis of the white-rot basidiomycete *Phanerochaete chrysosporium* grown under air and 100% oxygen, FEMS Microbiol. Let. 234 (2004) 111–116.

[24] M. Ringnér, What is principal component analysis?, Nat. Biotechnol. 26 (2008) 303–304.

[25] S.S. Doyle, Fungal proteomics: from identification to function. FEMS Microbiol. Lett. 321 (2011) 1–9.

[26] O. Bregar, S. Mandelc, F. Celar, B. Javornik, Proteome analysis of the plant pathogenic fungus *Monilinia laxa* showing host specificity, Food Technol. Biotechnol. 50 (2012) 326–333.

[27] D. Salvachúa, A.T. Martínez, M. Tien, M.F. López-Lucendo, F. García, V. de Los Ríos, M.J. Martínez, A. Prieto, Differential proteomic analysis of the secretome of *Irpex lacteus* and other white-rot fungi during wheat straw pretreatment, Biotechnol. Biofuels 6 (2013) 115.

[28] K. Kroll, V. Pähtz, O. Kniemeyer, Elucidating the fungal stress response by proteomics, J. Proteomics 97 (2014) 151–163.

[29] J.M.P.F. Ferreira de Oliveira, L.H. de Graaff, Proteomics of industrial fungi: trends and insights for biotechnology, Appl. Microbiol. Biotechnol. 89 (2011) 225–237.

[30] X. Yang, J.-Y. Sun, J.-L. Guob, X.-Y. Weng, Identification and proteomic analysis of a novel gossypol-degrading fungal strain, J. Sci. Food Agric. 92 (2012) 943–951.

[31] J. Fujii, Y. Ikeda, Advances in our understanding of peroxiredoxin, a multifunctional, mammalian redox protein, Redox Rep. 7 (2002) 123–130.

Mechanism study of alachlor biodegradation by *Paecilomyces marquandii* with proteomic and metabolomic methods.

Rafał Szewczyk, Adrian Soboń, Mirosława Słaba, Jerzy Długoński*

*Department of Biotechnology and Industrial Microbiology, Institute of Microbiology, Biotechnology and Immunology, Faculty of Biology and Environmental Protection, University of Łódź, Banacha 12/16, 90-237 Łódź, Poland, tel. +4842 635 44 65, Fax. +4842 665 58 18, jdlugo@biol.uni.lodz.pl

SUPPORTING MATERIAL

Contents

Table S-1. Multiple reaction monitoring (MRM) MS/MS scan mode – compound dependant parameters applied in the screening method.

Q1	Q3	dwell time (ms)	id	DP	EP	CE	CXP
185	97	5	3-Phosphoglycerate	-50	-10	-22	-10
101	57	5	Acetoacetate	-50	-10	-15	-10
403.6	79	5	Acetyl-CoA	-50	-10	-60	-10
173	129	5	Aconitate	-50	-10	-8	-10
426	79	5	ADP	-100	-10	-60	-10
145.1	101	5	a-Keto-glutarate/Adipate	-50	-10	-21	-10
346.1	79	5	AMP	-70	-10	-43	-10
175	115	5	Ascorbate	-50	-10	-17	-10
506	159	5	ATP	-100	-10	-45	-10
191	111	5	Citrate	-50	-10	-13	-10
339	241	5	F26BP/G16BP	-50	-10	-20	-10
115	71	5	Fumarate/Maleate	-50	-10	-15	-10
259	79	5	G1P/G6P/F1P/F6P	-60	-10	-35	-10
193	113	5	Glucoronate	-60	-10	-22	-10
89	59	5	Glyceraldehyde	-50	-10	-10	-10
185	79.1	5	Glycerate-2-P	-50	-10	-30	-10
93	57	5	Glycerol	50	10	12	10
171	79	5	Glycerol-3-P	-50	-10	-22	-10
181.1	137.1	5	Homovanillate	-50	-10	-12	-10
89	43	5	Lactate	-50	-10	-20	-10
133	115	5	Malate	-50	-10	-20	-10
103	59	5	Malonate	-50	-10	-15	-10
425.6	79	5	Malonyl-CoA	-50	-10	-62	-10
117	73	5	Methylmalonate/Succinate	-50	-10	-12	-10
147.1	59	5	Mevalonate	-50	-10	-19	-10
89	61	5	Oxalate	-50	-10	-18	-10
131	87	5	Oxaloacetate	-50	-10	-9	-10
167	79	5	PEP	-50	-10	-31	-10
73	55	5	Propionate	-50	-10	-20	-10
87	43	5	Pyruvate	-50	-10	-12	-10
565.1	323	5	UDP-glucose/UDP-galactose	-60	-10	-30	-10
579	403	5	UDP-glucuronate	-50	-10	-28	-10

Table S-2. Full set of Mascot and BLAST protein id search results after 120h of the P. marquandii control culture. Mascot algorithm matching - protein scores greater than 73 are significant ($p < 0.05$). Delta-BLAST algorithm - the lower the E-value (closer to zero), the more significant is the match. Green – identified (high score and/or high sequence coverage), yellow – functionally assigned by delta-BLAST (with low Mascot score), white – unidentified (very low Mascot score).

Spot ID.	Mascot search result							DELTA-BLAST Results
	Best Protein Accession	Mass [Da]	Calc. pI	Peptides Matched	Seq. Cov.	Score	Best Protein Description	
167	gi|511008026	87992				41	hypothetical protein HMPREF1544_03925 [*Mucor circinelloides* f. *circinelloides* 1006PhL]	No match
174	gi|471569154	94445				44	putative beta-glucosidase 1 precursor protein [*Eutypa lata* UCREL1]	No match
193/194	gi|358058207	72974				29	hypothetical protein E5Q_02659 [*Mixia osmundae* IAM 14324]	No match
196	gi|23894273	1401				9	SSU1 protein [*Saccharomyces cerevisiae*]	No match
200	gi|154320359	19709				40	predicted protein [*Botryotinia fuckeliana* B05.10]	No match
208	gi|396489610	108166				34	hypothetical protein LEMA_P089070.1 [*Leptosphaeria maculans* JN3]	No match
213	gi|521582664	93600				7	hypothetical protein PFL1_05814 [*Pseudozyma flocculosa* PF-1]	No match
227	gi|521585597	126585				44	hypothetical protein PFL1_03029 [*Pseudozyma flocculosa* PF-1]	No match
239	gi|310793840	101748				25	F-box domain-containing protein [*Colletotrichum graminicola* M1.001]	No match
249/247	gi|358398002	54863	5.47	31	50%	194	ATP synthase beta chain mitochondrial precursor [*Trichoderma atroviride* IMI 206040]	[cd01133] F1- ATP synthase beta subunit, nucleotide-binding domain; E=0e+00
	gi|400595077	55284	5.26	29	45%	171	ATP synthase beta chain [*Beauveria bassiana* ARSEF 2860]	[cl08258] ATP synthase alpha/beta chain, C-terminal domain; E=2.38e-33
	gi|471567117	54831	5.46	25	38%	159	putative atp synthase beta mitochondrial precursor protein [*Eutypa lata* UCREL 1]	[cl18399] ATP synthase alpha/beta family, beta-barrel domain; E=5.22e-19 [PRK09280] F0-F1 ATP synthase subunit beta; Validated;E=0e+00
250	gi|325092938	6030				16	conserved hypothetical protein [*Ajellomyces capsulatus* H88]	No match
252	gi|85096905	104082				35	hypothetical protein NCU07082 [*Neurospora crassa* OR74A]	No match
260	gi|171687114	24558				13	hypothetical protein [*Podospora anserina* S mat+]	No match
267	gi|530464730	1055				13	hypothetical protein CGLO_13888 [*Colletotrichum gloeosporioides* Cg-14]	No match
273	gi|387594736	5913				19	hypothetical protein NEQG_00530 [*Nematocida parisii* ERTm3]	No match
274	gi|336377750	5777				19	hypothetical protein SERLADRAFT_374663 [*Serpula lacrymans* var. *lacrymans* S7.9]	No match
281							no match	No match
287	gi|154310718	3693				12	predicted protein [*Botryotinia fuckeliana* B05.10]	No match
293	gi|393237102	6062				7	hypothetical protein AURDEDRAFT_45010, partial [*Auricularia delicata* TFB-10046 SS5]	No match
304	gi|401837510	44664				33	SLU7-like protein [Saccharomyces kudriavzevii IFO 1802]	No match
305	gi|82828	3374				37	ribosomal protein L15.e - fission yeast (Schizosaccharomyces pombe) (fragment)	No match
314	gi|322697295	35337	6.49	30	51%	105	Transaldolase [*Metarhizium acridum* CQMa 102]	[cd00957] transaldolases including both TalA and TalB; E=2.63e-176 [PTZ00411] transaldolase-like protein; Provisional; E=5.88e-152
	gi|322712191	34600	6.86	27	34%	105	transaldolase [*Metarhizium anisopliae* ARSEF 23]	
	gi|399165577	35653	5.64	20	29%	105	probable transaldolase [*Claviceps purpurea* 20.1]	
317	gi|363750480	6967				18	hypothetical protein Ecym_3136 [*Eremothecium cymbalariae* DBVPG#7215]	No match
319	gi|74620637	172929				17	RecName: Full=Pentafunctional AROM polypeptide; Includes: RecName: Full=3-dehydroquinate synthase; Short=DHQS; Includes: RecName: Full=3-phosphoshikimate 1-carboxyvinyltransferase; AltName: Full=5-enolpyruvylshikimate-3-phosphate synthase; Short=EPS	No match
321	gi|240280489	33573	4.83	23	51%	246	Stress protein DDR48 [*Ajellomyces capsulatus* H143]	[PRK12678] transcription termination factor Rho; Provisional; E=3.38e-04
	gi|154277766	32925	4.57	18	46%	237	Hypothetical protein HCAG_05184 [*Ajellomyces capsulatus* NAm1]	
	gi|13591791	31617	4.95	17	40%	229	mold-specific protein MS95 [*Ajellomyces capsulatus*]	
323	gi|530480609	1774				12	hypothetical protein CGLO_00011 [*Colletotrichum gloeosporioides* Cg-14]	No match
334	gi|406607769	34985				26	37S ribosomal protein S28, mitochondrial [*Wickerhamomyces ciferrii*]	No match
341	gi|302892809	34444	6.14	18	33%	151	predicted protein [*Nectria haematococca* mpVI 77-13-4]	[cd01337] glyoxysomal and mitochondrial malate dehydrogenases; E=0e+00 [PLN00106] malate dehydrogenase; E=1.30e-143
	gi|322695422	34218	6.46	17	29%	151	malate dehydrogenase precursor [*Metarhizium acridum* CQMa 102]	
	gi|531862512	43794	9.21	20	30%	151	malate dehydrogenase [*Ophiocordyceps sinensis* CO18]	

347	gi|169626276	5160				21	hypothetical protein SNOG_16424 [*Phaeosphaeria nodorum* SN15]	No match
353	gi|471899015	82929				37	Vacuolar protein sorting-associated protein 53 homolog [*Rhizoctonia solani* AG-1 IB]	No match
364	gi|531866468	36308				68	outer mitochondrial membrane protein porin [*Ophiocordyceps sinensis* CO18]	[cd07306] voltage-dependent anion channel of the outer mitochondrial membrane; E=1.10e-86 [pfam01459] eukaryotic porin; E=1.14e-80
374	gi|169607182	7121				13	hypothetical protein SNOG_06647 [*Phaeosphaeria nodorum* SN15]	No match
386	gi|154293126	48581				39	hypothetical protein BC1G_14515 [*Botryotinia fuckeliana* B05.10]	No match
390	gi|408394064	3838				13	hypothetical protein FPSE_06506 [*Fusarium pseudograminearum* CS3096]	No match
398/397	gi|46111661	69438				37	hypothetical protein FG02712.1 [*Fusarium graminearum* PH-1]	No match
401	gi|393244696	13072				30	tubulin binding cofactor A [*Auricularia delicata* TFB-10046 SS5]	No match
402	gi|406864210	140262				12	phosphoinositide phosphatase [*Marssonina brunnea* f. sp. '*multigermtubi*' MB_m1]	No match
417	gi|512202826	42678				11	hypothetical protein GLAREA_12408 [*Glarea lozoyensis* ATCC 20868]	No match
420	gi|254584456	17265				67	ZYRO0F13706p [*Zygosaccharomyces rouxii*]	No match
422	gi|396497374	141326				46	hypothetical protein LEMA_P002700.1 [*Leptosphaeria maculans* JN3]	No match
443	gi|388580531	58519				25	S-adenosyl-L-methionine-dependent methyltransferase [*Wallemia sebi* CBS 633.66]	No match
447	gi|116200005	26035				39	predicted protein [*Chaetomium globosum* CBS 148.51]	No match
448	gi|354546034	9943				20	hypothetical protein CPAR2_204060 [*Candida parapsilosis*]	No match
451	gi|70984978	16922	7.77	12	60%	265	nucleoside diphosphate kinase [*Aspergillus fumigatus* Af293]	[cd04413] nucleoside diphosphate kinase group I (NDPk_I)-like; E=5.04e-91
	gi|471560787	16736	7.77	11	41%	265	putative nucleoside diphosphate kinase protein [*Eutypa lata* UCREL1]	[pfam00334] nucleoside diphosphate kinase; E=5.36e-88
	gi|30315965	16898	7.82	11	56%	263	RecName: Full=Nucleoside diphosphate kinase; Short=NDP kinase; AltName: Full=AnNDK; Short=NDK	
453	gi|267931127	97739				20	trehalose-6-phosphate phosphorylase [*Beauveria bassiana*]	No match
454	gi|380478802	18135				20	hypothetical protein CH063_13103 [*Colletotrichum higginsianum*]	No match
465	gi|171694085	17464				39	hypothetical protein [*Podospora anserina* S mat+]	No match
472	gi|340519078	12201	4.72	5	23%	103	Predicted protein [*Trichoderma reesei* QM6a]	[DUF3759] protein of unknown function; E=1.93e-35
474	gi|530542000	76376				40	dna-directed rna polymerase i subunit [*Nosema apis* BRL 01]	No match
478	gi|406867499	52191				47	26S proteasome subunit RPN7 [*Marssonina brunnea* f. sp. '*multigermtubi*' MB_m1]	No match
480	gi|408389209	146308				11	hypothetical protein FPSE_11127 [*Fusarium pseudograminearum* CS3096]	No match
482	gi|471570119	11219				61	putative acyl binding protein [*Eutypa lata* UCREL1]	No match
783	gi|393212376	46981				11	hypothetical protein FOMMEDRAFT_162215 [*Fomitiporia mediterranea* MF3/22]	No match
491	gi|452842345	57750				11	hypothetical protein DOTSEDRAFT_53432 [*Dothistroma septosporum* NZE10]	No match
498	gi|302887142	94579				18	predicted protein [*Nectria haematococca* mpVI 77-13-4]	No match
499	gi|225678993	81798				10	3-phytase [*Paracoccidioides brasiliensis* Pb03]	No match
500	gi|539438359	59787				10	hypothetical protein EPUS_08122 [*Endocarpon pusillum* Z07020]	No match
507	gi|440493441	3948				19	hypothetical protein THOM_1120, partial [*Trachipleistophora hominis*]	No match

Table S-3. Full set of Mascot and BLAST protein id search results after 120h of the P. marquandii culture containing alachlor (50 mg L^{-1}). Mascot algorithm matching - protein scores greater than 73 are significant ($p < 0.05$). Delta-BLAST algorithm - the lower the E-value (closer to zero), the more significant is the match. Green – identified (high score and/or high sequence coverage), yellow – functionally assigned by delta-BLAST (with low Mascot score), white – unidentified (very low Mascot score).

Spot ID.	Mascot search results							DELTA-BLAST Results
	Best Protein Accession	Mass [Da]	Calc. pI	Peptides Matched	Seq. Cov.	Score	Best Protein Description	
160	gi|531865828	72449	5.70	32	32%	410	heat shock 70 kDa protein [*Ophiocordyceps sinensis* CO18]	[cd11733] nucleotide-binding domain of human HSPA9, *Escherichia coli* DnaK, and similar proteins; E=0e+00
	gi|322701734	73112	5.68	40	41%	368	heat shock 70 kDa protein precursor [*Metarhizium acridum* CQMa 102]	[PRK00290] molecular chaperone DnaK; Provisional; E=0e+00

	gi|322706829	73386	5.68	37	40%	367	heat shock 70 kDa protein [*Metarhizium anisopliae* ARSEF 23]	
163	gi|387538371	70470				35	heat shock protein 70 [*Blumeria graminis* f. sp. tritici]	No match
189	gi|322700211	62929	5.38	33	38%	155	phosphoglycerate mutase, 2,3-bisphosphoglycerate-independent [*Metarhizium acridum* CQMa 102]	[PRK05434]phosphoglyceromutase; Provisional; E=0e+00
	gi|322708166	63375	5.49	33	39%	155	2,3-bisphosphoglycerate-independent phosphoglycerate mutase (iPGM) [*Metarhizium anisopliae* ARSEF 23]	[Superfamily] cl17463, BPG-independent PGAM N-terminus (iPGM_N)
	gi|346326764	58747	5.25	26	27%	125	phosphoglycerate mutase, 2,3-bisphosphoglycerate-independent [*Cordyceps militaris* CM01]	
190	gi|254572409	20800				42	hypothetical protein [*Komagataella pastoris* GS115]	No match
201	gi|358399574	56475	6.26	25	28%	153	peroxisomal catalase [*Trichoderma atroviride* IMI 206040]	[cd08157] fungal catalases similar to yeast catalases A and T; E=0e+00
	gi|6014693	57211	6.79	21	29%	123	catalase isozyme P [*Ajellomyces capsulatus*]	[COG0753] catalase; E=0e+00
	gi|24528587	56849	6.50	14	21%	123	catalase [*Paracoccidioides brasiliensis*]	
223	gi|531866883	55138	5.33	33	57%	146	ATP synthase beta chain [*Ophiocordyceps sinensis* CO18]	[cd01133], F1 ATP synthase beta subunit, nucleotide-binding domain; E=0e+00
	gi|399171671	55040	5.48	23	41%	129	H+-transporting ATP synthase beta chain [*Claviceps purpurea* 20.1]	[Cdd:pfam00306] ATP synthase alpha/beta chain, C terminal domain; E=1.32e-31
	gi|440638891	55382	5.46	28	41%	117	ATP synthase subunit beta, mitochondrial [*Pseudogymnoascus destructans* 20631-21]	[Cdd:pfam02874] ATP synthase alpha/beta family, beta-barrel domain; E=3.60e-19
								[PRK09280] F0-F1 ATP synthase subunit beta; Validated; E=0e+00
238/242	gi|399170765	47165	5.39	15	35%	288	probable enolase (2-phosphoglycerate dehydratase) [*Claviceps purpurea* 20.1]	[cd03313] enolase; E=0e+00
	gi|477534317	47183	5.23	12	30%	264	enolase [*Colletotrichum orbiculare* MAFF 240422]	[PLN00191] enolase; E=0e+00
	gi|212537563	47395	5.39	13	30%	171	enolase/allergen Asp F 22 [*Talaromyces marneffei* ATCC 18224]	
256	gi|322696440	52422	8.43	29	29%	198	Phosphoglycerate kinase [*Metarhizium acridum* CQMa 102]	[cd00318] phosphoglycerate kinase (PGK); E=0e+00
	gi|322704254	44347	6.69	27	36%	198	Phosphoglycerate kinase [*Metarhizium anisopliae* ARSEF 23]	[Superfamily] cl00198, phosphoglycerate kinase (PGK)
	gi|302886659	44613	5.43	21	38%	129	predicted protein [*Nectria haematococca* mpVI 77-13-4]	
268	gi|322702591	39769	5.53	20	34%	109	cyanide hydratase [*Metarhizium anisopliae* ARSEF 23]	[cd07564] nitrilases, cyanide hydratase (CH)s, and similar proteins (class 1 nitrilases); E=2.75e-119
	gi|88766405	39768	5.63	20	34%	109	cyanide hydratase [*Metarhizium anisopliae*]	
275	gi|346322842	42559				68	vacuolar protease A precursor [*Cordyceps militaris* CM01]	[cd05471] pepsin-like aspartic proteases; E=3.95e-97
								[pfam00026] eukaryotic aspartyl protease; E=1.54e-119
285	gi|225559211	36835	8.26	16	28%	80	NADP-dependent glycerol dehydrogenase [*Ajellomyces capsulatus* G186AR]	[cd06660] aldo-keto reductases; E=7.51e-78
	gi|261204493	37322	6.28	15	30%	80	aldehyde reductase I [*Ajellomyces dermatitidis* SLH14081]	
	gi|239614213	37350	6.43	15	29%	80	aldehyde reductase I [*Ajellomyces dermatitidis* ER-3]	
286	gi|429862698	36234	6.25	33	55%	366	glyceraldehyde-3-phosphate dehydrogenase [*Colletotrichum gloeosporioides* Nara gc5]	[pfam02800] glyceraldehyde 3-phosphate dehydrogenase, C-terminal domain; E=7.93e-100
	gi|530477121	36248	6.25	31	55%	335	glyceraldehyde-3-phosphate dehydrogenase [*Colletotrichum gloeosporioides* Cg-14]	[pfam00044] glyceraldehyde 3-phosphate dehydrogenase, NAD binding domain; E=9.57e-80
	gi|477536372	36232	6.24	30	51%	333	glyceraldehyde-3-phosphate dehydrogenase [*Colletotrichum orbiculare* MAFF 240422]	[COG0057] glyceraldehyde-3-phosphate dehydrogenase/erythrose-4-phosphate dehydrogenase; E=0e+00
295	gi|302884358	39125	5.24	13	27%	139	fructose-bisphosphate aldolase [*Nectria haematococca* mpVI 77-13-4]	[PRK09197] fructose-bisphosphate aldolase; Provisional; E=0e+00
	gi|342871910	37275	5.24	10	21%	127	hypothetical protein FOXB_15150 [*Fusarium oxysporum* Fo5176]	[Superfamily] cl17181, fructose/tagarose-bisphosphate aldolase class II
	gi|475673861	39633	5.44	10	20%	127	Fructose-bisphosphate aldolase [*Fusarium oxysporum* f. sp. *cubense* race 4]	
304	gi|389747275	123885				30	hypothetical protein STEHIDRAFT_167739 [*Stereum hirsutum* FP-91666 SS1]	No match
307	gi|322697295	35337	6.49	38	51%	207	transaldolase [*Metarhizium acridum* CQMa 102]	[cd00957] transaldolases including both TalA and TalB; E=2.63e-176
	gi|322712191	34600	6.86	35	44%	195	transaldolase [*Metarhizium anisopliae* ARSEF 23]	
	gi|531856223	35087	6.86	34	49%	194	Transaldolase [*Ophiocordyceps sinensis* CO18]	[PTZ00411] transaldolase-like protein; Provisional; E=5.88e-152
311	gi|322697295	35337	6.49	30	39%	76	transaldolase [*Metarhizium acridum* CQMa 102]	[cd00957] transaldolases including both TalA and TalB; E=2.63e-176
	gi|322712191	34600	6.86	28	41%	76	transaldolase [*Metarhizium anisopliae* ARSEF 23]	
	gi|399165577	35653	5.64	23	29%	76	probable transaldolase [*Claviceps purpurea* 20.1]	[PTZ00411] transaldolase-like protein; Provisional; E=5.88e-152
313	gi|336464274	39807				43	mitochondrial Cytochrome c peroxidase [*Neurospora tetrasperma* FGSC 2508]	No match
314	gi|67539148	30223	4.85	16	28%	161	hypothetical protein AN5744.2 [*Aspergillus nidulans* FGSC A4]	[cd11309] fungal 14-3-3 protein domain; E=2.80e-138
	gi|46108718	27506	4.94	14	22%	161	hypothetical protein FG01241.1 [*Fusarium graminearum* PH-1]	[Superfamily] cl02098, 14-3-3 domain
	gi|70991439	30085	4.74	16	35%	161	14-3-3 family protein [*Aspergillus fumigatus* Af293]	
323/4	gi|302654183	20680	4.83	15	20%	202	conserved hypothetical protein [*Trichophyton verrucosum* HKI 0517]	[PRK12678] transcription termination factor Rho; Provisional; E=0.01
	gi|530473648	32195	4.45	20	47%	187	hypothetical protein CGLO_06169 [*Colletotrichum gloeosporioides* Cg-14]	[PRK08581] N-acetylmuramoyl-L-alanine amidase; Validated; E=0.03
	gi|261196113	40526	6.85	32	46%	186	mold-specific protein [*Ajellomyces dermatitidis* SLH14081]	
325	gi|451845560	86771				46	hypothetical protein COCSADRAFT_165126 [*Bipolaris sorokiniana* ND90Pr]	No match
344	gi|465796311	66213				39	unnamed protein product [*Malassezia sympodialis* ATCC 42132]	No match
384	gi|401888325	27630	7.64	15	40%	75	L-xylulose reductase [*Trichosporon asahii* var. *asahii* CBS 2479]	[cd05352] mannitol dehydrogenase (MDH)-like, classical (c) SDRs; E=1.03e-119
								[PRK05557] 3-ketoacyl-(acyl-carrier-protein) reductase;

								Validated; E=1.81e-52
391	gi|399170748	23636				36	probable MET14-ATP adenosine-5`-phosphosulfate 3`-phosphotransferase [*Claviceps purpurea* 20.1]	No match
392	gi|242210763	153303				34	predicted protein [*Postia placenta* Mad-698-R]	No match
396	gi|346327419	26911	6.02	14	32%	139	triosephosphate isomerase [*Cordyceps militaris* CM01]	[cd00311] triosephosphate isomerase (TIM); E=8.40e-111
	gi|315042127	27047	5.59	12	30%	110	triosephosphate isomerase [*Arthroderma gypseum* CBS 118893]	
	gi|302672679	26429	6.10	6	10%	104	hypothetical protein SCHCODRAFT_71461 [*Schizophyllum commune* H4-8]	
417	gi|310791594	19059				61	hypothetical protein GLRG_02292 [*Colletotrichum graminicola* M1.001]	No match
423	gi|46124419	23107				72	RS7_NEUCR 40S ribosomal protein S7 [*Fusarium graminearum* PH-1]	[pfam01251] ribosomal protein S7e; E=5.11e-101
426	gi|322707797	24900				65	manganese superoxide dismutase [*Metarhizium anisopliae* ARSEF 23]	[pfam02777] iron/manganese superoxide dismutases, C-terminal domain; E=1.25e-50 (super family) cl02809; E=1.92e-33 [COG0605] superoxide dismutase; E=7.09e-90
445	gi|340518075	18835				47	acetyltransferase [*Trichoderma reesei* QM6a]	No match
446	gi|361124833	21389				53	putative Peptidyl-prolyl cis-trans isomerase, mitochondrial [*Glarea lozoyensis* 74030]	No match
460	gi|340518820	14822	10.12	16	48%	86	histone H2B [*Trichoderma reesei* QM6a]	[smart00427] histone H2B; E=4.30e-49 [Superfamily] cl00074, histone H4
	gi|358385634	14836	10.12	16	48%	86	hypothetical protein TRIVIDRAFT_92198 [*Trichoderma virens* Gv29-8]	
	gi|51701481	14789	10.16	14	42%	86	RecName: Full=Histone H2B	
488	gi|169866979	38595				32	hypothetical protein CC1G_12126 [*Coprinopsis cinerea* okayama7#130]	No match
496	gi|340519078	12201	4.72	7	23%	82	predicted protein [*Trichoderma reesei* QM6a]	[DUF3759] protein of unknown function; E=1.93e-35
	gi|322708039	11859	5.02	7	57%	81	phosphoglycerate mutase family protein, putative [*Metarhizium anisopliae* ARSEF 23]	
	gi|531861288	11406	5.87	4	33%	81	hypothetical protein OCS_04883 [*Ophiocordyceps sinensis* CO18]	
501	gi|354548424	10273				38	hypothetical protein CPAR2_701720 [*Candida parapsilosis*]	No match
504	gi|449548976	97320				37	hypothetical protein CERSUDRAFT_81259 [*Ceriporiopsis subvermispora* B]	No match
507	gi|401888325	27630				48	L-xylulose reductase [*Trichosporon asahii* var. *asahii* CBS 2479]	No match
509	gi|389747275	123885				29	hypothetical protein STEHIDRAFT_167739 [*Stereum hirsutum* FP-91666 SS1]	No match
510	gi|85096905	104082				36	hypothetical protein NCU07082 [*Neurospora crassa* OR74A]	No match
514	gi|465796311	66213				39	unnamed protein product [*Malassezia sympodialis* ATCC 42132]	No match
518	gi|388851491	17286				39	probable ribosomal protein L24.e.A, cytosolic [*Ustilago hordei*]	No match
524	gi|449548609	174362				39	hypothetical protein CERSUDRAFT_111891 [*Ceriporiopsis subvermispora* B]	No match
528	gi|240278303	134994				45	p150 dynactin NUDM [*Ajellomyces capsulatus* H143]	No match